

Conf-820839--5

BNL 31970

BNL--31970

DE83 002221

ION TIME-OF-FLIGHT SPECTROSCOPY: KRYPTON CHARGE-STATE SPECTRA AS A FUNCTION OF PHOTON EXCITATION ENERGY NEAR THE K EDGE\*

J.B. Hastings

National Synchrotron Light Source

Brookhaven National Laboratory

Upton, New York 11973

MASTER

V.O. Kostroun

Nuclear Science and Engineering Program and

School of Applied and Engineering Physics

Cornell University

Ithaca, New York 14853

NOTICE

PORTIONS OF THIS REPORT ARE ILLEGIBLE. IT

has been reproduced from the best available copy to permit the broadest possible availability.

ABSTRACT

In this experiment, we have recorded the charge state distribution resulting from atomic rearrangement following the creation of the inner shell vacancies in krypton atoms. Intense, highly collimated, monochromatic and tunable x-ray radiation available at the CHESSE synchrotron radiation facility at Cornell was used to photoionize krypton atoms in a gas jet target, and a time-of-flight spectrometer was used to record the ions in different charge states formed after photoionization. Charge state spectra were recorded at below, at the "peak" in the K edge and above the edge. Below the edge, charge states +4 to +7 were observed with appreciable intensity, while at, and above the edge, the charge states ranged from +4 to +10.

DISCLAIMER

This report was prepared as an account of work sponsored by an agency of the United States Government. It is not to be distributed outside the agency. The views and opinions contained herein do not necessarily state or reflect those of the United States Government or any agency thereof. The views and opinions of the authors expressed herein do not necessarily state or reflect those of the United States Government or any agency thereof.

\*Work supported by the U.S. Department of Energy.

EMB

## I. INTRODUCTION

The value of x-ray absorption spectroscopy as a method for determining the local atomic environment is well established. For a number of reasons, both theoretical and experimental, reference absorption spectra of isolated atoms would be highly desirable. Yet apart from the K absorption spectra of the noble gases (closed shell systems) deep core absorption spectra of isolated atoms are almost non-existent. The need for such spectra is exemplified by a recent calculation by Manson and Inokuti<sup>1</sup> who have shown that the free atom spectral strength (which in turn is proportional to the photoionization cross section) has a near threshold structure which has an appreciable magnitude (e.g., 24% for Ar) and appears to be common to many atoms. The variation is due to one of the many electron optical effects of atomic fields, and the result has an important implication in the study of solids by photoemission, electron energy-loss spectroscopy or EXAFS where such near threshold structure may be attributable to solid state effects.

Similarly, absorption spectra of simple atomic aggregates consisting of two, three, four, or more atoms of the same type would be valuable in investigating the theoretical aspects of EXAFS calculations. Clusters of a few atoms, e.g.,  $\text{Ge}_n(n=2-6)$ <sup>2</sup> or  $\text{Au}_n(n=2-7)$ <sup>3</sup> are formed in vapors at sufficiently high temperatures. However, the measurement of deep core absorption spectra of very low density gases, vapors or even monatomic layers of foreign atoms on surfaces is very difficult because of the very penetrating nature of electromagnetic radiation in the x-ray region and the small number of atoms involved, typically of the order of  $10^{11}$  to  $10^{14}$  atoms/cm<sup>2</sup>. Furthermore, unavoidably scattered radiation as well as photoelectrons and Auger electrons contribute significantly to the overall background radiation in the x-ray or electron detectors used, often resulting in data with poor signal to noise ratios. Because of this, x-ray absorption spectra of say metallic vapors, vapors of molecular compounds or medium to high Z impurity atoms on surfaces are non-existent or very difficult to obtain.

In conventional absorption spectroscopy, the number of photons transmitted through a sample is recorded as a function of incident photon energy. However, absorption spectra can also be obtained by recording the radiations (x-rays or Auger electrons) emitted in the de-excitation of the inner shell vacancy created in photoabsorption, a technique particularly useful for recording absorption spectra of dilute samples. When dealing with very dilute samples, such as atomic or molecular vapors of an element or compound at temperatures well below the boiling point, detection of ions formed in photoionization as a function of incident photon energy provides yet another means for recording absorption spectra. Since these low energy ions can be detected with very high efficiency compared to x-rays or Auger electrons, they provide a particularly useful label signaling the absorption of a photon by an isolated system.

The labeling is quite distinct, since the de-excitation of an atom with an inner shell vacancy results in a highly ionized ion on a time scale comparable to the lifetime of the initial core hole. To detect the ions formed, we have designed and constructed a time-of-flight (TOF) charge spectrometer of the Wiley-McLaren type<sup>4</sup> which can be used to record absorption spectra of gases, metal vapors and atoms on surfaces by measuring the total number of ions produced as a function of incident photon energy. [The total number of ions recorded is directly related to the number of vacancies formed at a given photon energy, which in turn depends on the value of the absorption coefficient  $\mu(E)$ .]

## II. THEORETICAL BACKGROUND

As an atom with an inner shell vacancy de-excites, the excitation energy is carried away by a series of x-ray, Auger and Coster-Kronig transitions, all of which cause the transfer of inner shell vacancies to outer shells on a time scale comparable to the lifetime of the core vacancy. (X-ray emissions leave the charge state of an ion unaltered while non-radiative (electron) emission increases the charge state by one.) A series of nonradiative transitions can therefore give rise to an atom with an appreciable number of its outer electrons missing. The process of vacancy transfer from the initial core hole to final multiple ionized atom is referred to as "vacancy cascade". The process is mostly associated with

free atoms in which case it has been well established. For example, a K vacancy in krypton gives rise to an experimentally observed charge distribution which ranges from 1 to 12 and has a mean of  $6^5$ .

The process of vacancy cascade, which occurs on a time scale of the order of  $10^{-15}$  sec is negligible compared to the ion collection time in the TOF charge spectrometer,  $\sim 10^{-6}$  sec, and provides the basis for the measurement of absorption spectra of low density vapors and gases by generating ions and ion distributions characteristic of the inner shell vacancy produced.

The inner shell vacancy cascade has numerous ramifications, many of which are based on the following experimental results: Carlson and White<sup>6</sup> have measured the relative abundance and recoil energy spectra of fragment ions resulting from vacancy cascades following creation of deep core holes in elements which form a part of large molecules such as  $C_2H_5I$ ,  $CH_3CD_2I$  and  $Pb(CH_3)_4$ . In particular, the study on tetramethyl lead showed that when the molecule was irradiated by Mo K x-rays, complete molecular decomposition was observed. Furthermore, the high charge state that one would normally anticipate for lead (from studies on mercury atoms) had been reduced to the most probable charge of one by electron pickup from methyl groups. As a result of this, the hydrocarbons were completely destroyed. The very low recoil energy of the lead ion observed ( $< 0.05$  eV) suggests that the Coulomb repulsion between the central lead atom and its symmetrically located methyl groups tend to cancel out the recoil as the highly charged molecular ion explodes from a common center. This was borne out in recoil calculations in which the methyl groups were placed about the lead atom in a tetrahedral arrangement. For equally charged methyl groups, the net calculated recoil for lead was zero. To estimate the effect of an asymmetric charge distribution, one of the methyl groups was left uncharged in the calculation, and this small degree of asymmetry generated a lead ion with a recoil energy more than five times greater than observed experimentally.

### III. EXPERIMENTAL ARRANGEMENT

The experimental arrangement consists of a synchrotron radiation source, monochromator and TOF charge spectrometer. The monochromator, a Si(220) channel cut crystal with a weak link, provided monochromatic radiation into the A-2 hutch at the Cornell High Energy Synchrotron Source (CHESS).<sup>7</sup> With this arrangement, it is possible to get  $\sim 10^5$  photons/eV-mrad at the appropriate energy in a single pulse, 0.4 nsec wide every 2.56  $\mu$ sec.

The operation of the TOF spectrometer shown in Fig. 1 is as follows: a monochromatic synchrotron radiation pulse enters the spectrometer through a 0.25 mm Be window and passes through the source region where it creates ions by photoionization of gas atoms flowing from a small orifice, actually an electron microscope aperture 100  $\mu$ m in diameter. After passing through the source region, the radiation exits the spectrometer through an Al window 0.025 mm thick and impinges on a plastic scintillator which is coupled to a fast photomultiplier, PM, in Fig. 1. This detector provides a reference stop pulse to the time to amplitude converter (TAC) shown in the block diagram of Fig. 2. Ions of interest are propelled into the main acceleration region of the spectrometer, after which they enter the drift region with the same kinetic energy per unit charge. Since their velocity is proportional to  $(q/m)^{1/2}$ , ions of the same mass but different charge  $q$  arrive at a detector in a time proportional to  $(m/q)^{1/2}$ . The arrival of an ion at the detector (a channeltron) generates a signal which is used to start the time-to-pulse-height converter, and the total time of flight of the ion from its formation to arrival at the detector is therefore accurately known. For ions of the same mass, different charge states are obtained, and at each photon energy, the total number of ions and their charge and velocity distribution can be obtained.

As can be seen from Fig. 2, the detected ions are used as the start pulse and the reference pulse as the stop. Because there are so few ions produced, (typically 5 per second) this arrangement lets the TAC operate only when an event is detected and thus minimizes the dead time associated with the TAC cycle time that would occur if the reference pulse were used as the start. In this mode the slowest (lowest charge states) occur at the shortest time (time difference) between their arrival and the stop pulse.

Furthermore, because of the very few events and good time resolution flight times longer than the 2.56  $\mu$ sec pulse to pulse separation which appear in the spectrum as frame overlaps of pulses occurring at a time  $t = t_0 + n \times 2.56 \mu$ sec can be identified.

The TOF spectrometer is identical to that of Wiley and McLaren.<sup>4</sup> The first grid, G<sub>1</sub>, is at ground, the second, G<sub>2</sub>, at -63 volts and the drift region is set to -1512 volts (see Fig. 1). V<sub>1</sub>, the channeltron potential was typically set at -2300 volts. With a unity gain emitter-follower preamplifier, and 10<sup>8</sup> gain in the channeltron ion pulses of the order of 10 millivolts were obtained. The separation of the grids G<sub>1</sub> and G<sub>2</sub> is 0.2 cm, that between grid, G<sub>2</sub>, and the drift region 1.2 cm and the drift region is 40 cm long.

A liquid nitrogen trapped diffusion pump with an estimated effective pumping speed of 150  $\ell$ /sec pumped on the system. During data collection, the vacuum in the drift region was typically  $1 \times 10^{-5}$  Torr with a back pressure on the gas target jet a few tenths of a Torr.

Finally, the spectrometer was carefully aligned with respect to the incident photon beam whose intensity was monitored by a transmission ion chamber to normalize the measurements. Great care was taken to minimize the scattered radiation caused by the incident beam emphasizing on the grids. After doing so the theoretical K edge jump of 7.04 for Kr was routinely measured.

## EXPERIMENTAL RESULTS

Preliminary experiments have been carried out in Kr gas in the neighborhood of the K edge at 14325 eV. Two multichannel analyzer TOF spectra, one below threshold and one above threshold are shown in Figs. 3a and 3b respectively. The tentative charge state assignments are shown on these figures. A number of things can be clearly seen even in the raw data. First, above threshold, as expected, the higher charge states +8, +9, and +10 are much more intense than below threshold due to opening of the K-XY Auger channel. Second, the prompt pulse, coming from scattered radiation is much narrower than the ion peaks. Thus, the widths of the ion peaks are not due to intrinsic limits in the electronics, but rather are due to the mass spread of various krypton isotopes, the thermal energy spread of the ions and the TOF spread due to finite source width.

The initial stage of analysis has been completed and the total number of ions in charge states +4 to +9 has been determined. The detailed fits to these spectra which include the effects mentioned above are in progress. The results of the initial analysis are given in Fig. 4 where the integrated ion yield as a function of photon energy is plotted. The lines are just guides to the eye. The photon energy scale is calculated from the angle of the Si(220) monochromator and not a calibrated value. The value of the K edge jump,  $\gamma$ , is observed for all the charge states measured. In future measurements, we plan to investigate the charge state dependence of the various features of the Kr absorption spectrum as a function of photon excitation energy in order to determine the onset of double ionization, etc. To do so will require better statistics.

#### SUMMARY

A TOF spectrometer of the Wiley-McLaren design<sup>4</sup> has been constructed and tested at CHESS. Preliminary results on the photoionization of Kr gas are encouraging and detailed analysis of these data is in progress. Further studies on elemental vapors and solid surfaces are planned.

REFERENCES

1. S.T. Manson and M. Inokuti, "Near Threshold Structure in the Atomic K-Shell Spectra for Ionization by Photons or Fast Charged Particles" in Inner Shell and X-Ray Physics of Atoms and Solids, D.J. Fabian, H. Kleinpoppen and L.M. Watson Eds., (Plenum Press, New York 1981) p.273.
2. A. Kent and B.H. Strauss, *J. Chem. Phys.* 45, 822 (1966).
3. P. Sudrand, Thesis, Universite Paris Sud (Orsay, France) 1979 (to be published).
4. W.C. Wiley and L.H. McLaren, *Rev. Sci. Instr.* 26, 1150 (1955).
5. T.A. Carlson, W.E. Hunt and M.O. Krause, *Phys. Rev.* 151, 41 (1966).
6. T.A. Carlson and R.M. White, *J. Chem. Phys.* 48, 5191 (1968).
7. B.W. Batterman, *Nucl. Instrum. and Methods* 177, p.35 (1980).
8. E. Storm and H.I. Isreal, *Nuclear Data Tables Vol. A7*, p.565 (1970).

FIGURE CAPTIONS

- Fig. 1. Schematic of the TOF spectrometer.  $G_1$  and  $G_2$  are grids, set at ground and  $-63$  v respectively. The drift region is at  $-1512$  v and  $V_1$ , the bias on the channeltron  $-2300$  v. PM is the plastic scintillator - photomultiplier reference signal S is the strip collector for the signal.
- Fig. 2. Electronics block diagram. The components used are Ortec 485 amplifier, Ortec 551 single channel analyzer (SCA), and Ortec 457 time to amplitude converter (TAC).
- Fig. 3. a. Multichannel analyzer output below K threshold. Plotted is the counts as a function of channel number with the tentative charge state assignments.  
b. Same as (a) but above K threshold.
- Fig. 4. Integrated intensity as a function of photon energy for charge states  $+4$  to  $+9$ . The intensities have been normalized to  $2 \times 10^8$  monitor counts. The solid lines are guides to the eye.

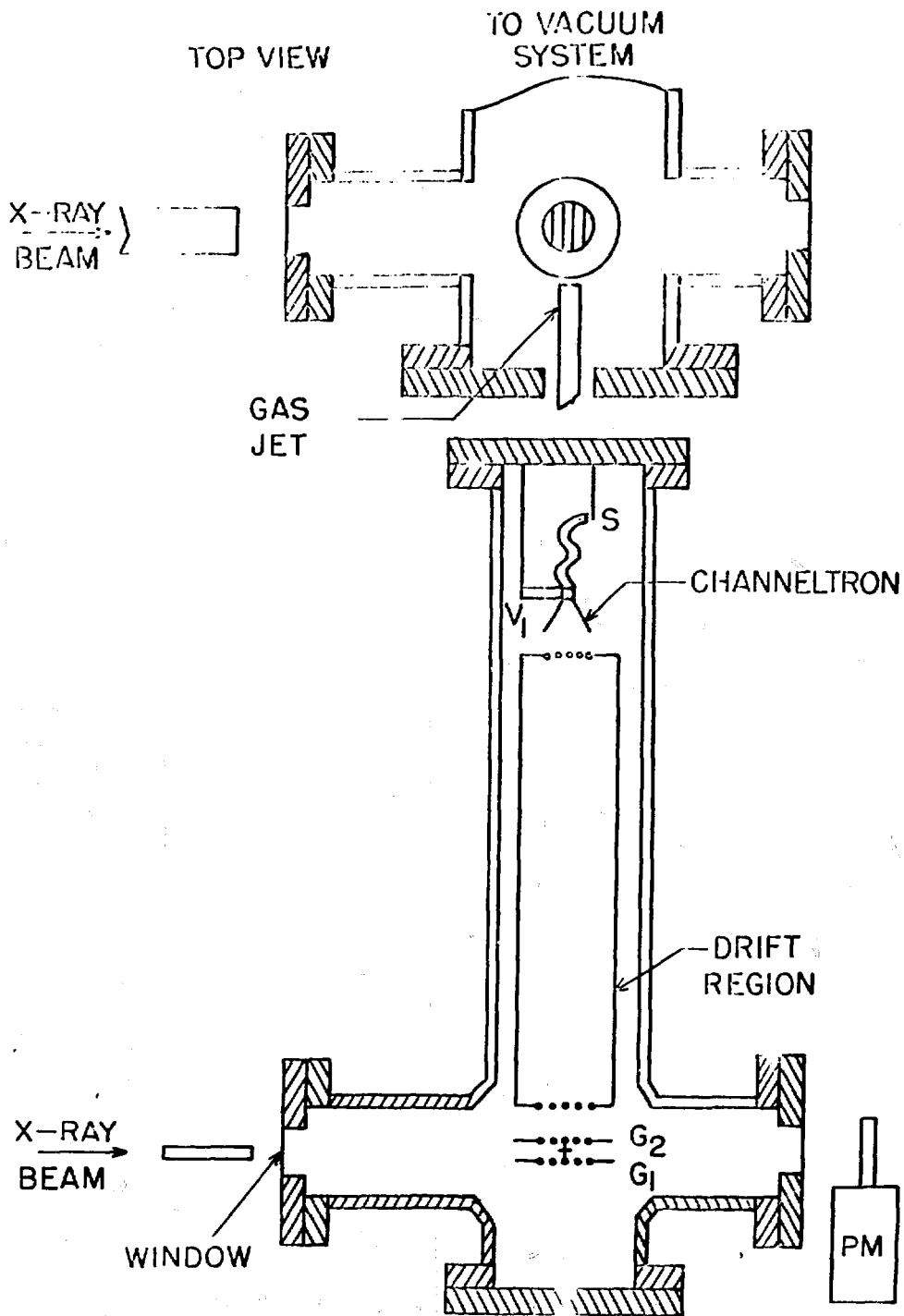


Fig. 1

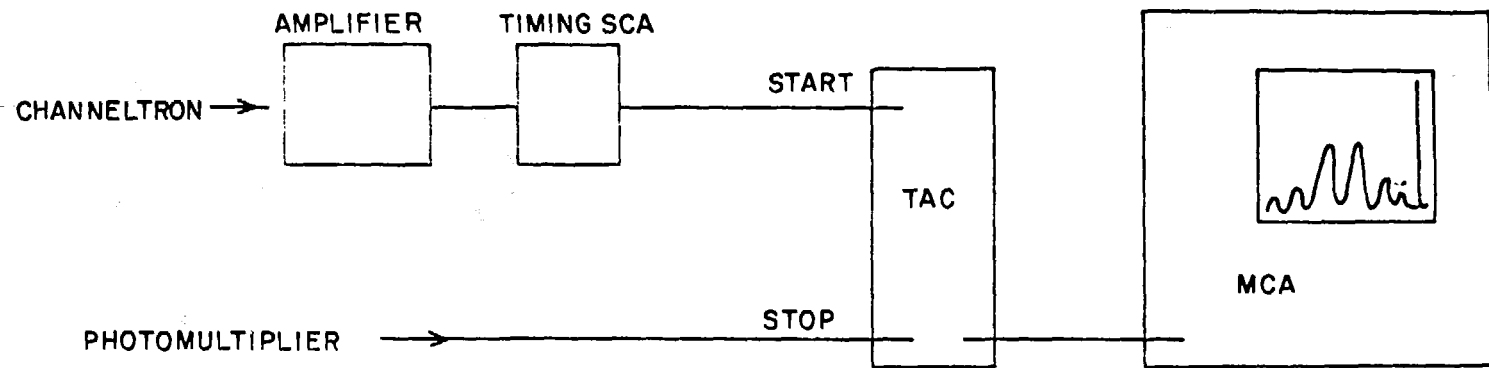


Fig. 2

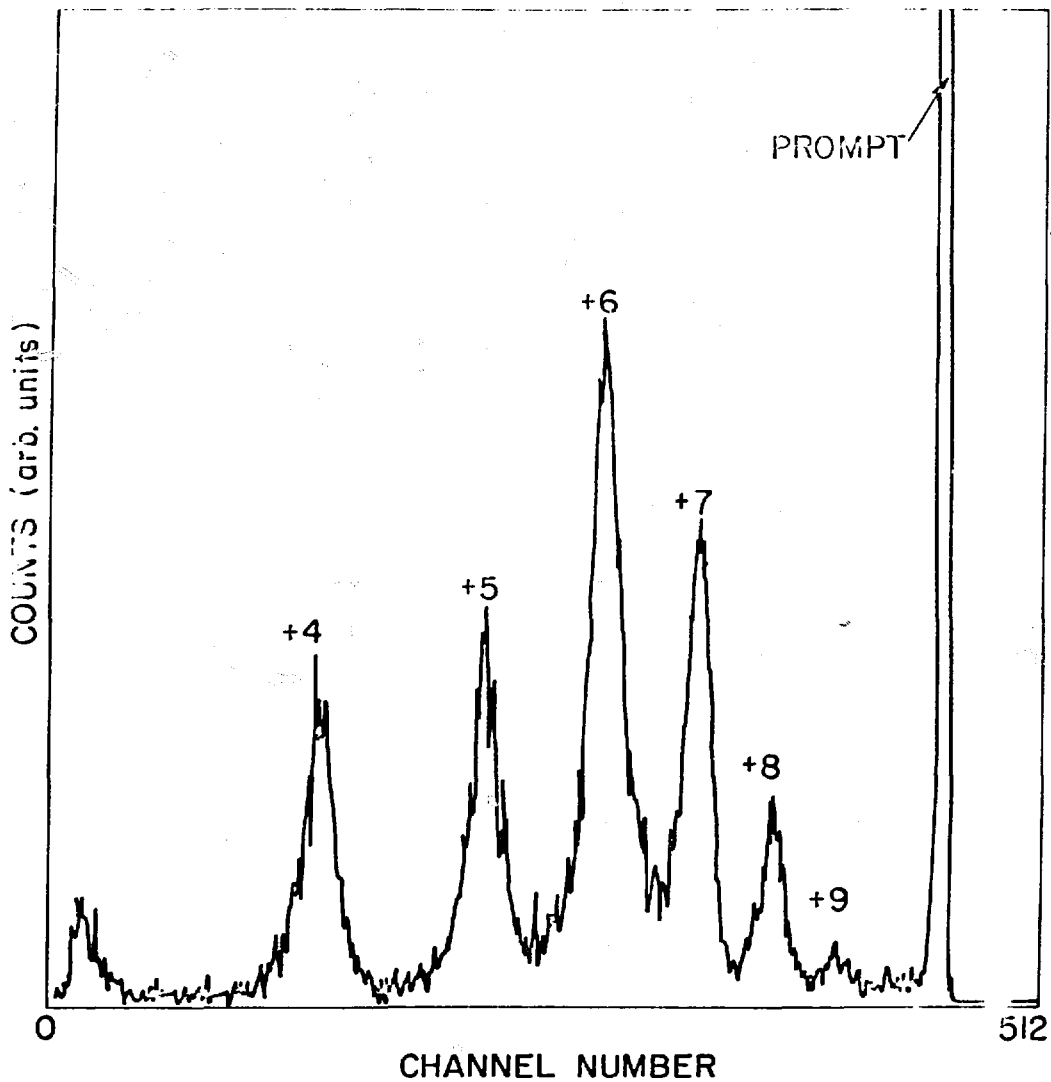


Fig. 3a'

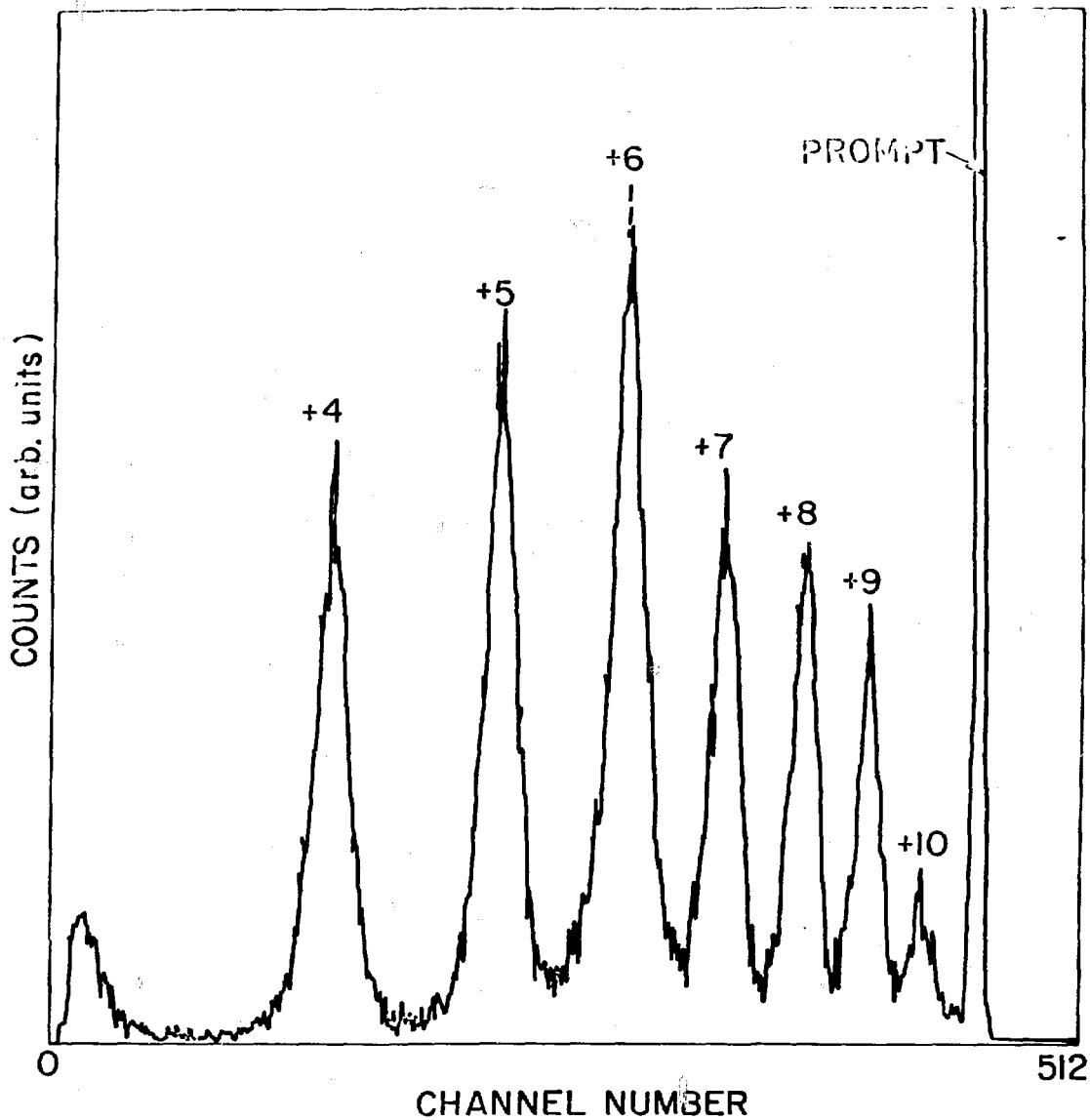


Fig. 3b

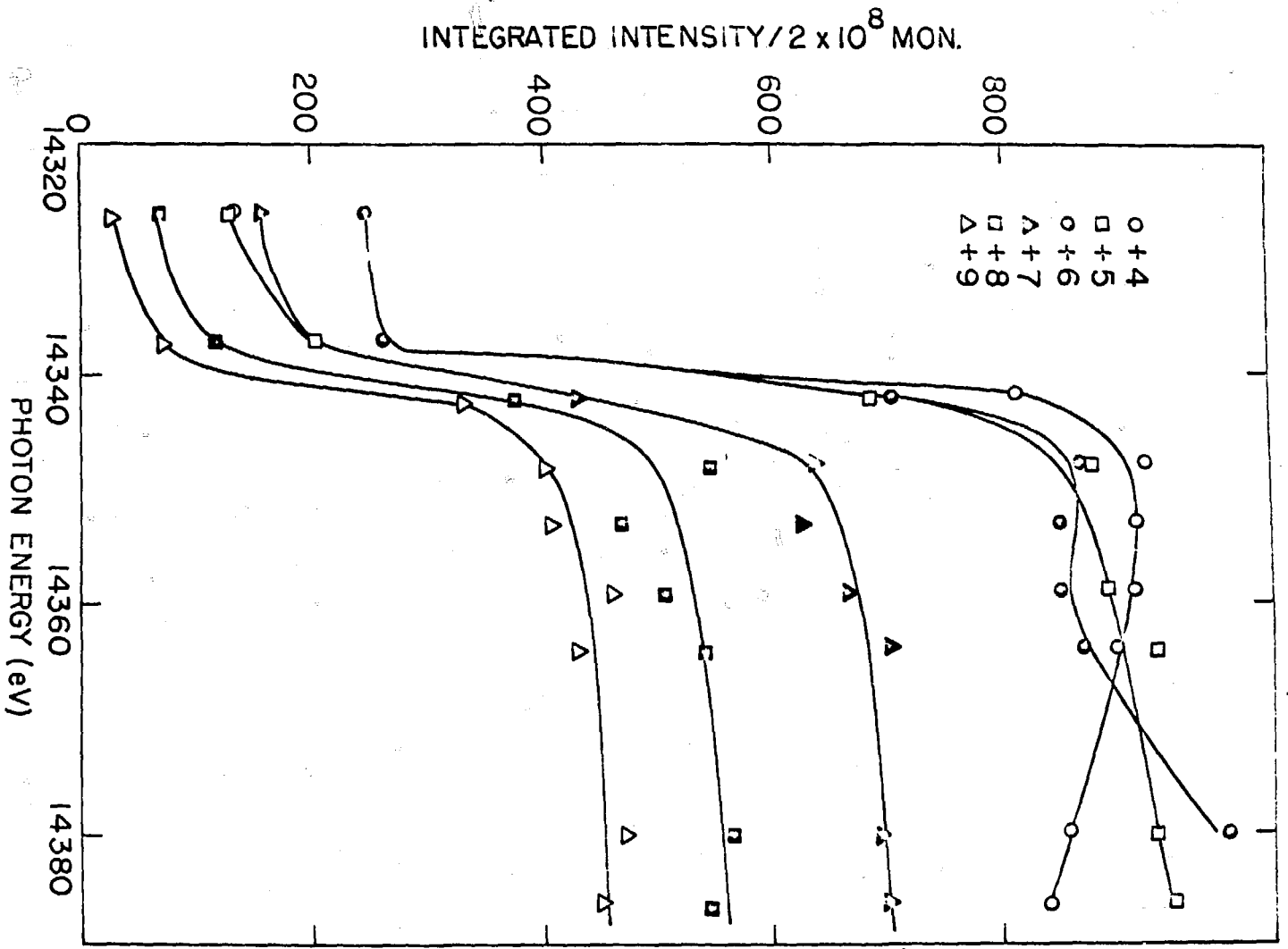


Fig. 4